Advances in Military Technology
Vol. 19, No. 1, 2024, pp. 55-69
ISSN 1802-2308, eISSN 2533-4123
DOI 10.3849/aimt.01855

Experimental and Numerical Validation of an Armor Plate Test Stand

K. Kosiuczenko*, P. Simiński, M. Gmitrzuk and M. Nowakowski

Military Institute of Armored and Automotive Technology, Sulejówek, Poland

The manuscript was received on 19 September 2023 and was accepted after revision for publication as research paper on 19 March 2024.

Abstract:

Nowadays military vehicles play an integral role in the transportation and protection of personnel and equipment ensuring safe and effective operations. The spectrum of threats ranges from high-velocity projectiles to the dangers posed by improvised explosive devices (IEDs). To evaluate the properties of individual materials, a stand for assessing the performance of vehicle armor plates under diverse condition was developed at the Military Institute of Armored and Automotive Technology (WITPIS). The test platform was designed to carry out multi-variant tests involving blast loading scenarios that impact the combat vehicle's chassis. The prepared testing procedure was proven through a series of tests using the Armox 500 plate. The achieved parameters were validated using a numerical model to confirm the acquired measurements.

Keywords:

blast load testing, protection plate, modelling techniques, numerical simulations

1 Introduction

Testing armor plates play critical role in safe military personnel and equipment operation [1-3]. These plates serve as an important protection tool against threats such as bullets, explosives, and shrapnels, directly impacting the used vehicles. Ensuring the effectiveness of armor through rigorous testing is not only a matter of protection, but also a key factor in mission success [4-6]. Military operations often take place in hostile environments [7-8], where the ability to withstand attacks is paramount. Properly tested armor provides the confidence that soldiers and equipment can perform effectively under such circumstances, reducing the risk of damage.

This study presents the results of experimental and numerical research carried out in the area of anti-mine resistance. The described tests were conducted at the Military

* *Krzysztof Kosiuczenko, Development Department, Military Institute of Armored and Automotive Technology, Okuniewska 1, 05-070 Sulejówek, Poland. Phone: +48 261 811 012, +48 261 811 073, E-mail: krzysztof.kosiuczenko@witpis.eu. ORCID 0000-0002-3097-5488.*

Institute of Armor and Automotive Technology for the purpose of designing new military vehicles. It was necessary to build a stand designed for evaluating the performance of the vehicle's armor plates under various conditions.

The test platform has the ability to carry out multi-variant tests of blast loading influencing chassis of the combat vehicle using various composition and mass of explosives. The structure consists of a metal frame, allowing the mounting of tested armor plate, as well as of numerous sensors used to record accelerations, displacements and deformations. Prior to the implementation of a new testing procedure, the experimental results were validated using an alternative method. This validation was carried out using computational methods, including numerical simulations, and comparing the results achieved with those obtained from the performed tests.

The applied numerical method, based on the FEM method (Finite Element Method), is an excellent tool allowing the detailed understanding of the test stand properties [9]. It can determine the design impact of installed equipment on the accuracy of the measurements. Despite the results of verification, numerical analysis is useful in test procedure improvement to design the optimal configuration, as well as to predict experimental outcomes before conducting the tests. This approach saves both time and costs generated by repeated experiments. It should be highlighted that FEM numerical simulation is a valuable tool to detect and identify sources of errors or inaccuracies that may affect the results of tests performed under complex measurement conditions, such as detonations.

The described FEM analysis is useful for a comprehensive understanding of the testing platform properties and the creation of an equivalent numerical model, enabling a quick and cost-effective verification of armor plates.

2 Description of Detonation Phenomena

Explosives, upon detonation, release an immense amount of energy, generating shockwaves that propagate at high supersonic velocities. The shock wave, generated as a result of the rapid burning of the material, begins to move in all directions, from the point of initiation until it encounters an obstacle (plate) [10].

The schematic diagram of the shock wave is shown in Fig. 1, where the explosive charge (W) is marked, distanced from the obstacle by the length (R). The shape of the pressure wave exhibits positive phase characterized by a rapid increase in pressure up to pressure P_{so} in a very short period of time. This is followed by negative phases decreasing below the ambient pressure (P_0), and then a slow rise to the ambient pressure level.

3 Validation of Developed Test Stand

3.1 Fabricated Test Stand

The developed stand for experimental tests is made of a steel frame enabling the installation of tested armor plates with maximum dimensions of 1 000 × 1 000 mm as shown in Figs 2 and 3. The plate is tightened around the entire perimeter with screwed flat bars in a specific optimal sequence [11] as shown in Fig. 2. A metal sling is placed above the plate to attached explosive charges.

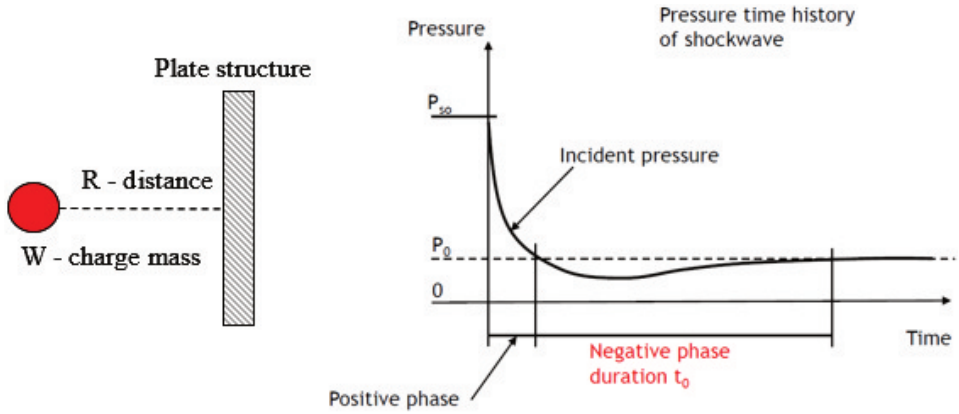

Fig. 1 Pressure-time history of pressure wave from explosion for a defined point of the tested structure

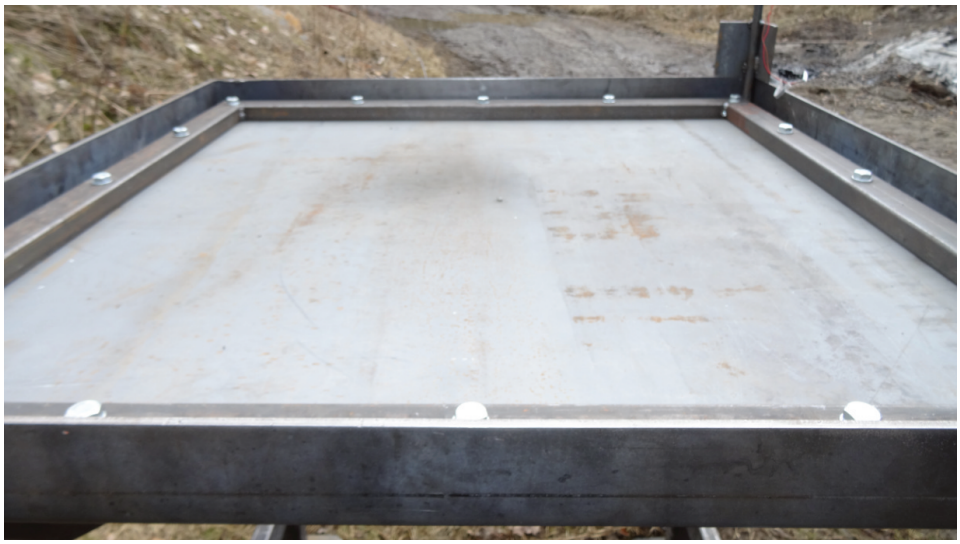

Fig. 2 Mounting method of armor plate on developed test stand

In order to observe the maximum deformation of the plate, a measuring comb and measuring rods were used. It should be highlighted that to certain extent, the measurements are inaccurate, because the maximum deformation occurs after the end of the entire experiment. This deformation might be influenced by subsequent interaction of the wave reflected from the ground, introducing uncertainties into the recorded data.

The installed acceleration sensors (Fig. 3) allow to monitor real time values of accelerations and displacements. These values were recorded using a multi-channel HIOKI recorder with a sampling rate of 20 kHz. In order to obtain additional useful information, the measurement channel was equipped with an additional acceleration sensor to record the velocity of the center of the stand compartment (in case the displacement sensor can be damaged). Such approach allows additional validation of the measured values.

The results of the experimental test (displacements and acceleration) were analyzed using the DIAdem software provided by National Instruments. The program has implemented tools to convert the acceleration recorded with the accelerometer into velocity and displacement. The displacement sensor which was additionally installed provides data to calculate derivatives of velocity and acceleration.

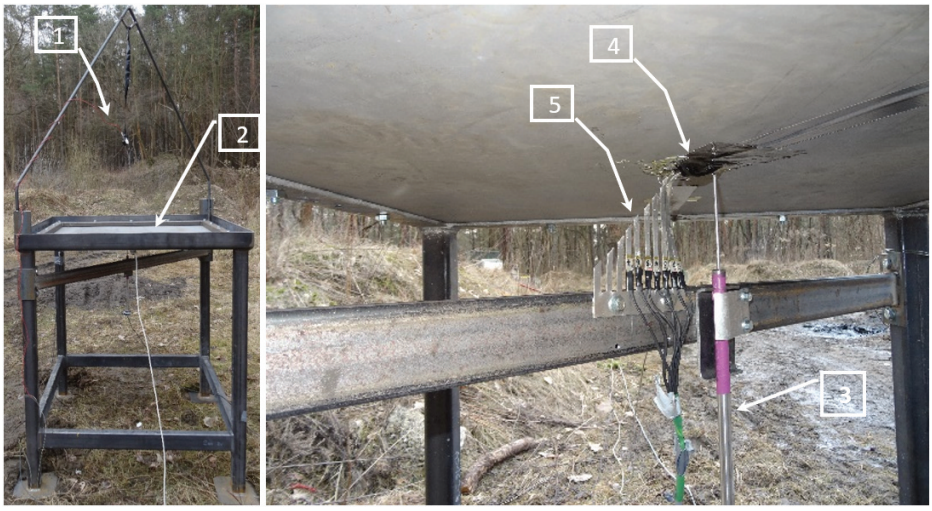

Fig. 3 Test stand: 1 - explosive; 2 - tested armor plate; 3 - bar displacement sensor; 4 - acceleration sensor; 5 - measuring comb

3.2 Test Setup for Experimental Purpose

The validation tests were performed by detonating different masses of plastic C4 placed above the plate made of Armox 500 steel with dimensions of 1 000 × 1 000 × 8 mm in the range of 25-100 mm. The presented variants are described in Tab. 1.

Tab. 1 Validation conditions of test stand

	Load mass [g]	Load distance [mm]
1.	25	300
2.		400
3.		500
4.	50	300
5.		400
6.		500
7.	100	500

ARMOX 500 is a specialized high-strength steel designed to provide exceptional protection against ballistic threats. It offers resistance to penetration and is widely used in military and protective applications like armored personnel carriers and tanks. Its capacity to absorb and dissipate energy from projectiles like bullets and fragments elevates crew safety during combat operations.

3.3 Experimental Results

The results of experimental tests for individual variants are shown in Figs 4-8. Fig. 4 shows the comparison of the velocities calculated from the acceleration sensor (ACC) and recorded from the displacement sensor (DISP): respectively for 25 g and 50 g of C4 material detonated at different distances from the center of the plate.

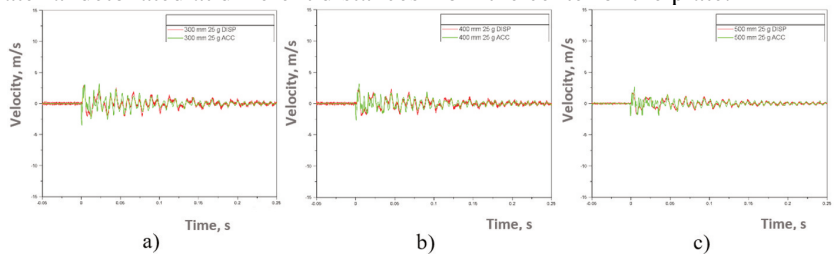

Fig. 4 Comparison of velocity calculated from acceleration sensor (ACC) and recorded from displacement sensor (DISP): for C4 weighing 25 g *detonated at a distance from the center of the plate:* 300 m *(a),* 400 mm *(b)* 500 mm *(c)*

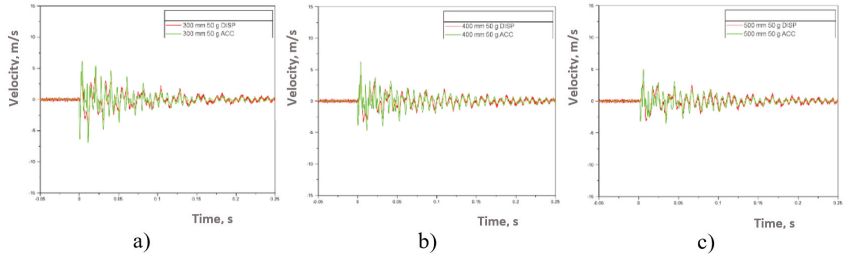

Fig. 5 Comparison of velocity calculated from acceleration sensor (ACC) and recorded from displacement sensor (DISP): for C4 weighing 50 g *detonated at a distance from the center of the plate:* 300 m *(a),* 400 mm *(b)* 500 mm *(c)*

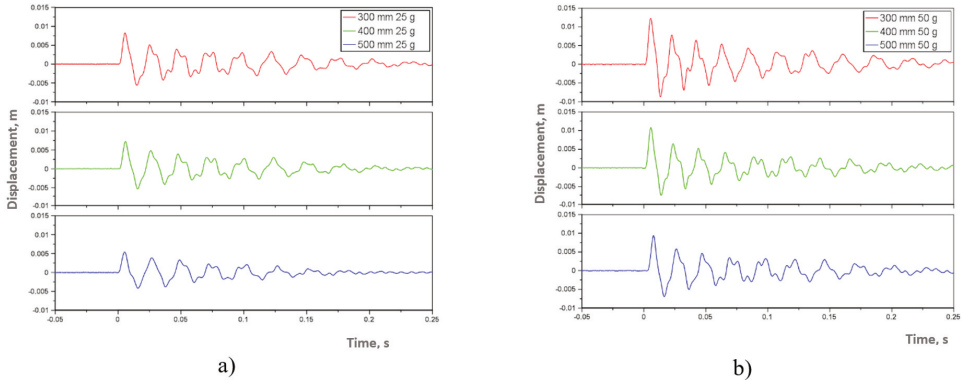

Fig. 6 Comparison of plate center displacement for: 25 g *C4 (a) and* 50 g *C4 (b), depending on the distance of the load from the plate*

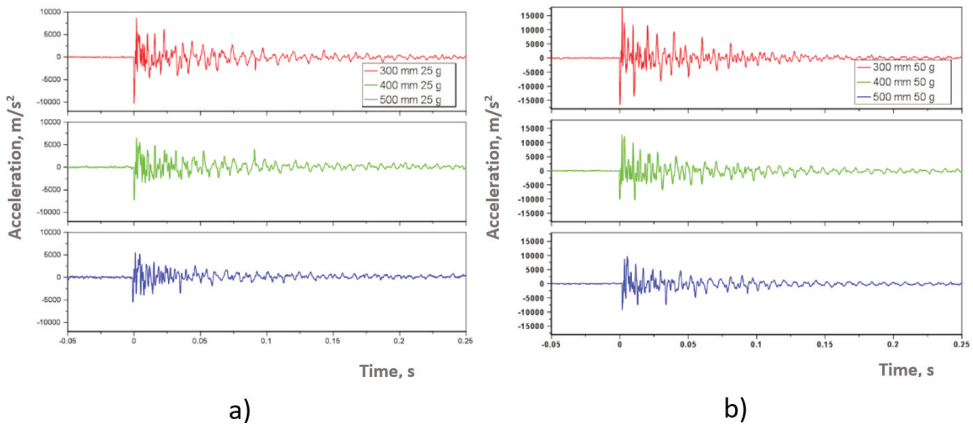

Fig. 7 Comparison of plate center acceleration for: 25 g *C4 (a) and* 50 g *C4 (b), depending on load distance from the center of plate compartment*

The results obtained from different sensors, especially displacements and accelerations (Fig. 7), show a high degree of similarity related to the waveform patterns and extreme values. It should be highlighted that both methods prove to be highly effective in determining the damping characteristics of energy-intensive systems. Due to the potential damage risk of measuring equipment during explosive testes, it is highly recommended to record both displacement and acceleration at the same time. This approach offers several advantages, including redundancy in data collection. If one set of equipment has a failure, the other can continue gathering critical information, preventing data loss.

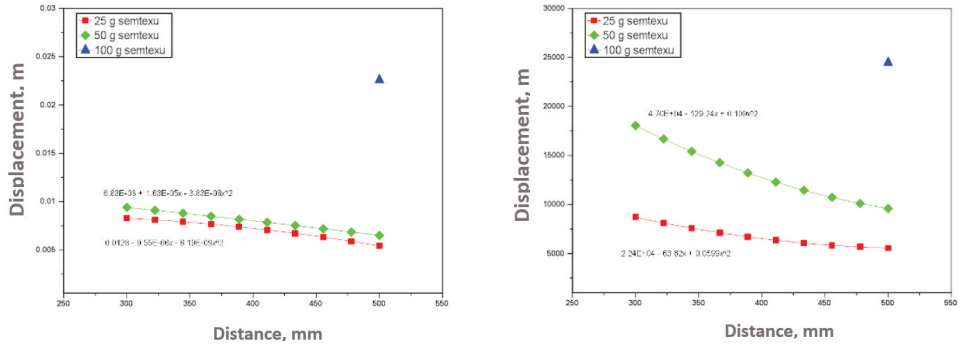

Fig. 8 Maximal values of displacement (a) and acceleration (b) of combustion center as a function of distance

In the tests of plates subjected to the pressure wave generated by the detonation of explosives, it is extremely important to properly prepare the method and the test stand. Due to the substantial energy involved, there is a risk of losing the ability to record certain parameters. Therefore, it is advisable to use multiple measurement methods, like accelerations and displacements, and perform initial equipment calibra-

tion to mitigate potential data loss. The displacement sensor is suitable for small plate displacements. In addition, these sensors are not very sensitive to interference from high-frequency vibrations generated in the plate. The acceleration sensor has no limits related to the maximum displacement of the plate, but the recorded results are strongly affected by the elastic wave generated in the plate as a result of the overpressure wave. A wave propagating at the speed of sound excites the acceleration sensor to periodically oscillate at high frequency. In order to eliminate this undesirable phenomena, various types of vibration dampers were used to suppress undesirable vibration components. Additionally, it is possible to perform spectral analysis; however, this requires additional software and it consumes time, as well as it may introduce additional errors due to the calculation algorithms.

The specific configuration from Tab. 1 was chosen for numerical analysis considering quality and comprehensiveness of the real test results. The developed numerical model considers the scenario involving a 50 g load positioned at the distance of 300 mm above the plate. It must imitate the same conditions as during the tests using ARMOX 500 steel plate with the dimensions of 1 000 × 1 000 × 8 mm. Moreover, the simulations used C4 explosive matching the material employed in the real scenario.

4 Numerical Model of Developed Stand

4.1 Numerical Modelling

The numerical model of the stand was developed using the finite element method using LS DYNA software. The LOAD_BLAST (LB) technique was used for the simulation, the core of which is a method similar to ConWep (ConWep is not built into LS DYNA). These techniques, similar to LOAD_BLAST_ENHANCED (LBE), are based on the use of an approximation of the experimental data set from the LLNL Explosives Handbook. The accuracy of this method has been thoroughly tested, and the error of mapping the actual pressure wave does not exceed 2-7 % [12].

Since the C4 charge was used in the experiment instead of the standard TNT, the masses were recalculated to obtain the calculated TNT charge mass corresponding to the actual C4 charge (the so-called equivalent mass). One of the approximation formulas known to researchers (1) was used for this purpose [12]

$$m_{\mathrm{TNT}} = m\frac{DCJ^2}{DCJ_{\mathrm{TNT}}^2} \tag{1}$$

where m_{TNT} – the mass of TNT equivalent [kg], m_{C4} – the mass of the load used (C4) [kg], DCJ – the Chapman-Jouguet detonation velocity [m/s].

Since the literature values of the detonation velocity for C4 are 8 193 m/s, while TNT is 6 900 m/s and taking into account Eq. (1), the mass of, for example, 50 g of C4 corresponds to 70 g of TNT.

The use of the ConWEP method is acceptable provided that the appropriate boundary conditions are met, for which the load cannot be placed too close or too far from the plate. This condition shows the pattern Hopkinson and Cranz [13]

$$\begin{cases} 0.147 < Z < 40 & \text{for spherical wave surface} \\ 0.178 < Z < 40 & \text{for hemispherical wave surface} \end{cases} \tag{2}$$

where the scaled distance Z is calculated according to the formula (3):

$$Z = \frac{R}{\sqrt[3]{m}} \tag{3}$$

where R – the distance between the center of the load and the center of the plate [m], m – the TNT equivalent mass [kg].

For the conditions specified for the experiment ($m = 25 \div 100$ g, $R = 300 \div 500$ mm), the value of Z was in the range of $Z = 0.65 \div 1.7$. It classifies it as a medium explosion distance (medium field) $Z = 0.4 \div 4$.

The schematic diagram of the physical model of the test stand is shown in Fig. 9 below.

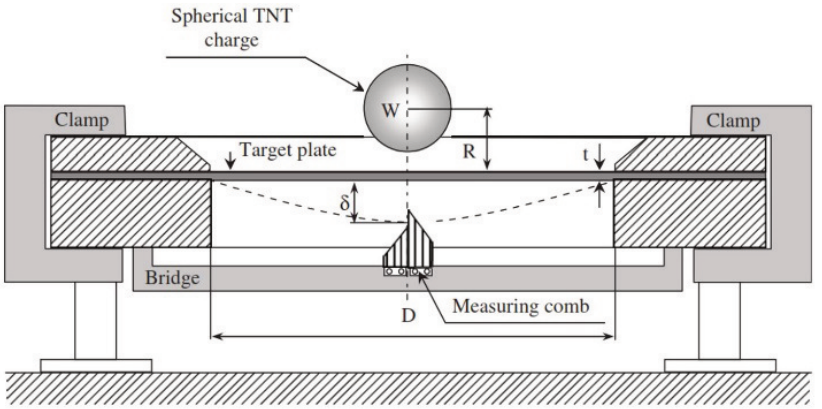

Fig. 9 Physical model of the test stand

Boundary conditions for the simulated test stand were achieved by placing translational constraints around the entire perimeter of the plate. In the numerical model, it was assumed that the initial conditions did not involve external forces affecting the plate (having influence on the initial state of the system). The gradual increase of the gravitational load occurred only at time $t = 0$, and was continued until reaching a stable state at time t = 0.2 s.

The plate geometry was described using the LS-PrePost automatic mesh generator with a regular finite elements cells (20 × 20 × 2 mm) maintaining the required side length ratio (max. 1:10). During the mesh generation process, the option to compact the mesh was not employed. This decision was made because there was no anticipation of plate perforations, significant deformations, or asymmetric stress concentrations that would require such mesh adjustments. The developed numerical model consists of 10 000 elements and 13 000 nodes (Fig. 10).Numerical Simulation Results

The developed FEM numerical model consisted of e.g. a dense grid of elements describing the tested plate. To imitate the material properties of the Armox 500 steel plate, the Johnson-Cook material model was used to describe all elements. The Johnson-Cook material model is commonly used in simulations of dynamic events, vehicle crash simulations, and blast simulations or ballistics. It is an empirical model that takes into account the strain rate, temperature, and plastic strain in the material. This formula takes into account the influence of strain rate and melting temperature and is given by [13, 14]

$$\sigma = \left(A + B\varepsilon^{n}\right)\left(1 + C\ln\dot{\varepsilon}^{*}\right)\left(1 - T_{\mathrm{m}}^{*}\right)$$
$$T^{*} = \frac{T - T_{0}}{T_{\mathrm{m}} - T_{0}} \tag{4}$$

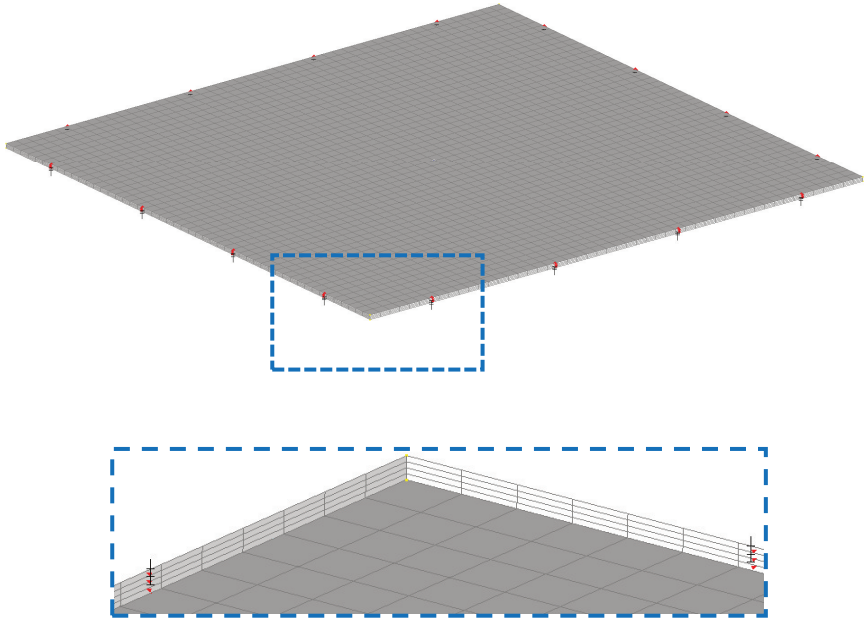

Fig. 10 Numerical model of tested plate with mesh structure including red constraints

where A, B, C, n, m – the material constants, T_{m} – the melting point, T_0 – the initial temperature, ε_p – the plastic strain, $\dot{\varepsilon}^{*}$ – the normal strain rate.

The JC model uses only a few material coefficients (A, B, C, n, m), which are determined experimentally. These coefficients (A, B, n) can be calculated from a static tensile or torsion test, or alternatively according to the dynamic methods.

Additional coefficients C and m are determined by dynamic methods, such as the Taylor or Hopkinson rod method. The JC model is popular in the literature, so all details describing material coefficients for Armox 500 steel can be found easily. Such parameters were used in the developed model.

The numerical model was built in the LS-DYNA simulation environment using the finite element method. Due to the nature of the simulated phenomena, the explicit option was used. According to good practice, the time step has been shortened to 0.67 of the nominal step (up to 2.15×10^{-7} s). To capture the complete explosion process and observe the damping of plate vibrations, recording was conducted for a duration of 0.25 seconds, with results being recorded at the intervals of 0.5 milliseconds. This recording scheme combine various data, including the following maps: displacement, velocity, acceleration, strain, and stress among other parameters (as a result of the postprocessing calculation). Selected stress maps are shown below (Figs 11 and 12).

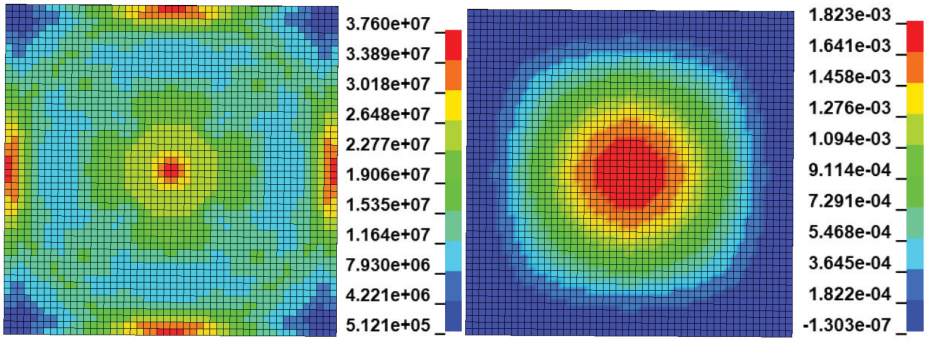

Fig. 11 Example of maps (for R = 300 mm, m = 50 g, t = 0.05 s): reduced stresses HMH [Pa] *– on the left and strains* [m] *– on the right*

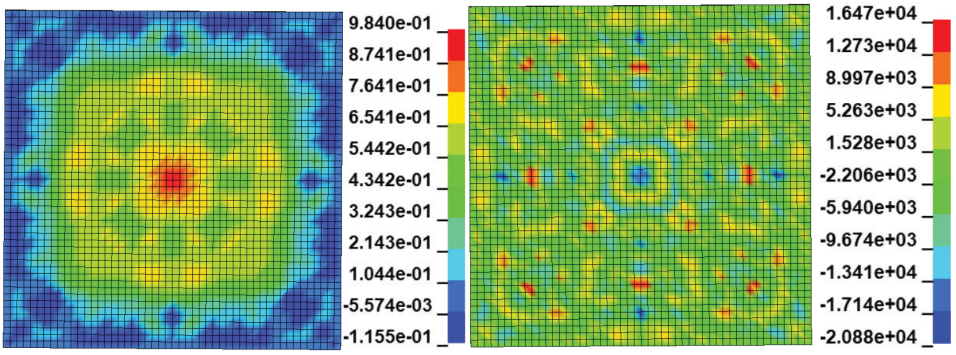

Fig. 12 Example maps (for R = 300 mm, m = 50 g, t = 0.05 s): velocities (perpendicular to the plate) [m/s] *– on the left and accelerations (perpendicular to the plate)* [m/s^2] *(for t = 0.05 s) – on the right*

Taking into consideration the nature of the data collected during the experiment, further analysis was conducted on the time courses of the aforementioned parameters, particularly focusing on the data obtained at the center of the plate. These waveform data were subsequently employed for the purpose of model validation, specifically concerning the scenario where R = 300 mm and m = 50 g (Figs 13-15).

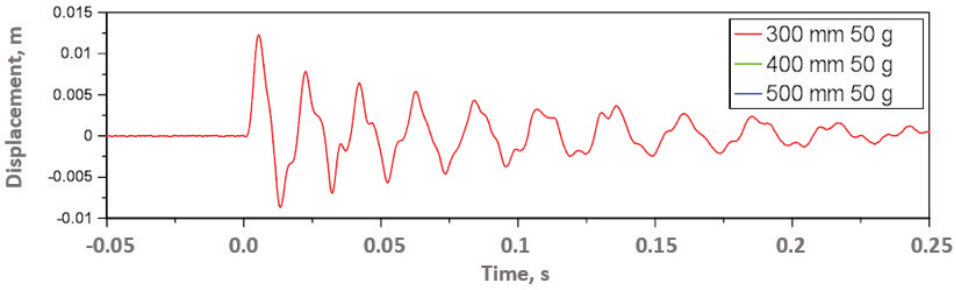

Fig. 13 Time-History of the plate center displacement obtained from the experiment.

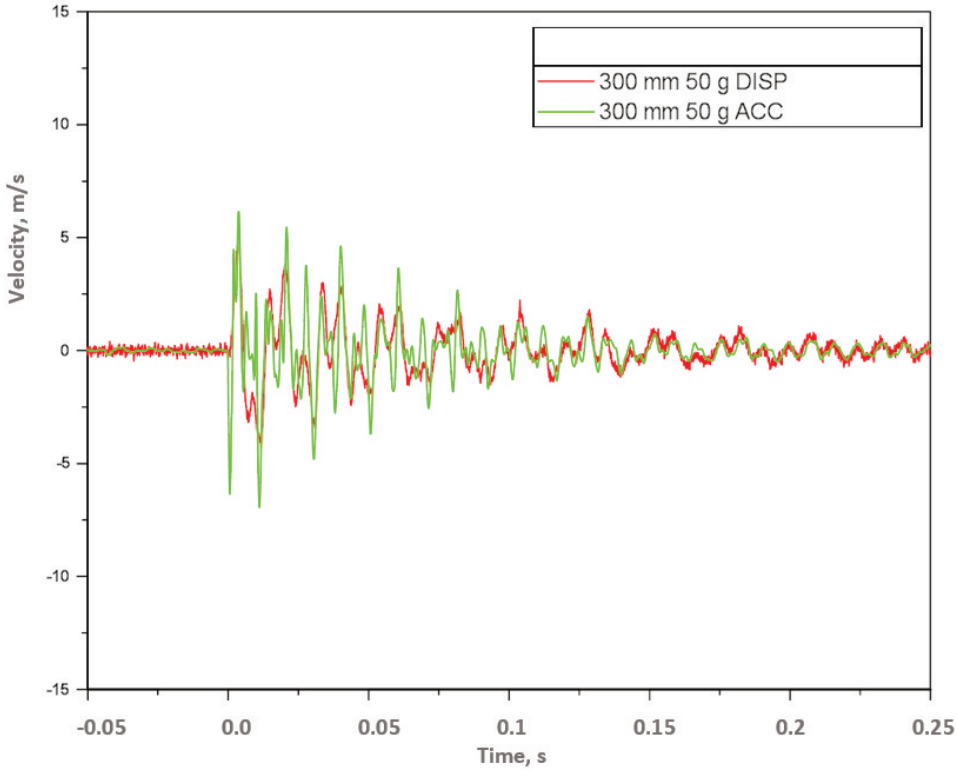

Fig. 14 Time-History of the plate center velocity (unit: 0.025 s*) obtained from the experiment*

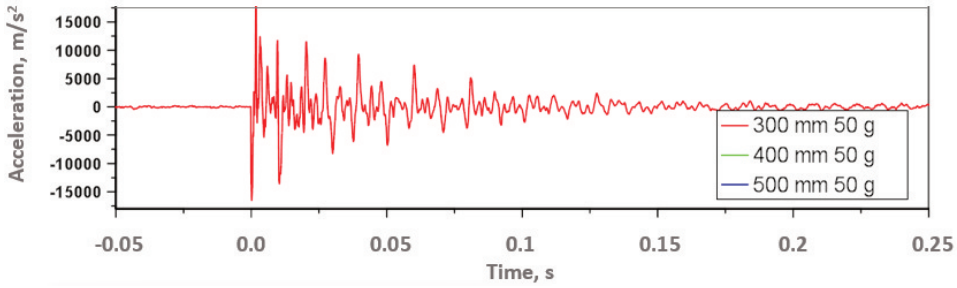

Fig. 15 Time-History of the plate center acceleration (unit: 0.025 s*) obtained from the experiment*

The above time-history data were compared with the results obtained from numerical calculations (Figs 16-18). The graphs corresponding to the node of the geometrical center of the front surface of the plate were used for the analysis. It is important to highlight the fact that in both experimental and numerical simulation results, the vertical axes have been inverted, and the explosion event occurs after the time t = 0.02 s, following a period during which the steel undergoes relaxation due to gravity load.

DOI 10.3849/aimt.01855

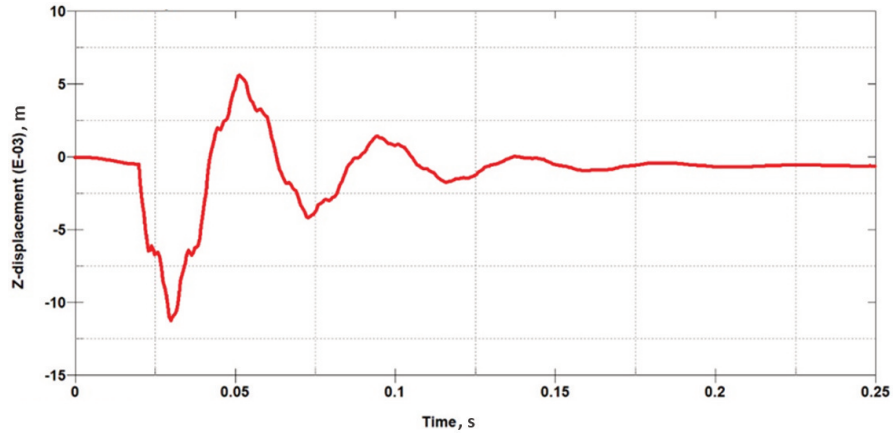

Fig. 16 Time-History of plate center displacement obtained from the simulation

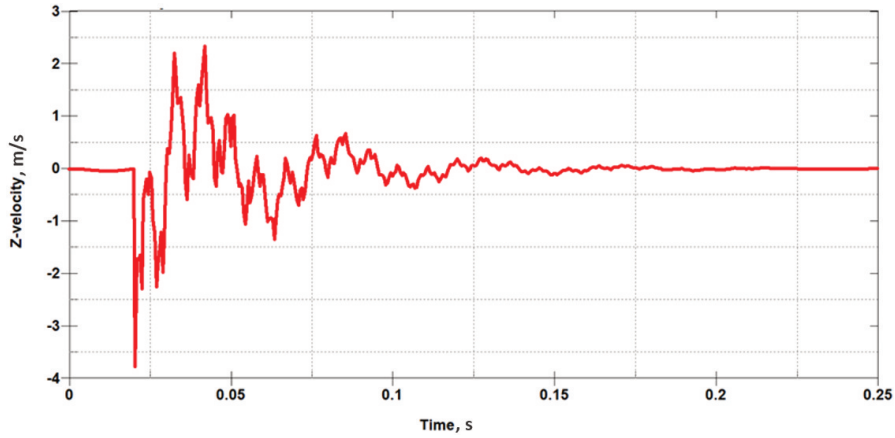

Fig. 17 Time-History of the plate center velocity obtained from the simulation

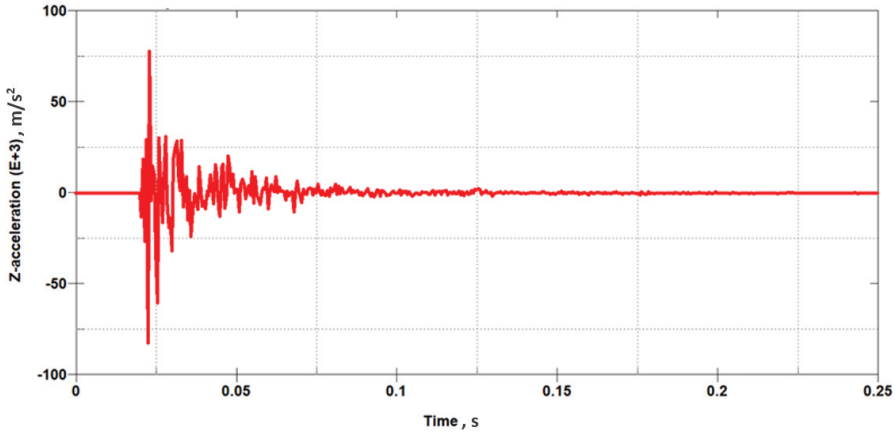

Fig. 18 Time-History of the plate center acceleration obtained from the simulation

5 Results and Discussion

To validate the testing procedure and the developed test stand, it is essential to compare the waveforms obtained during the experiment with those generated by equivalent numerical model. The recorded displacements in the simulation environment were approximately 10% smaller than those observed in carried out field tests.

The results shown in Tab. 2 confirm that the numerical model adequately captured the physical behavior of the test stand. The 10% difference in displacements observed between the numerical model and the experimental results closely aligns with the benchmark of 7% commonly reported in the literature for simulations of similar models. The obtained results prove that the experimental and numerical results are consistent confirming that the test stand was developed properly and the all measurements during the experiment were accurate.

Tab. 2 Comparison of the results obtained during experiment and simulations

Parameter	Ref.	Experiment	Simulation	Relative difference
Maximum displacement of the center of the plate	T_z [mm]	12.5	11.2	10%
Maximum plate center velocity	v_z [m/s]	4.8	3.77	20%
Maximum acceleration of the center of the plate	a_z [m/s^2]	17 000	77 000	–

It can be assumed that the differences between the results obtained through experimental and numerical methods arise from the combination of errors inherent in both numerical model and the measurement procedures. Despite the fact that the experimental data was accurately recorded, some differences, particularly in velocities and accelerations, suggested potential issues in measuring dynamic parameters. However, these dynamic parameters are less critical for ballistic plate strength analysis and therefore can be neglected.

6 Conclusions

Achieving an accurate representation of blast loading similar to the real-life scenarios, often requires full-scale field tests. To assess the performance of vehicle armor plates under diverse conditions, a testing platform was developed to carry out multi-variant blast loading test. This test stand allows enables to define the impact of various explosive compositions and weights on the combat vehicle's plates.

The fabricated structure is based on robust metal frame for mounting armor plates and multiple sensors for recording critical data, including accelerations and displacements. The testing procedure was validated comparing experimental results and an alternative method using numerical modeling. The results confirm the appropriateness of the test stand's development and the accuracy of the measurements acquired during the experimental phase.

Acknowledgement

The work was supported under research work no. 55.2022489.PL at the Military Institute of Armoured and Automotive Technology. This is an extension paper of 17th International Conference on Materials and Technologies for Defense and Security

References

[1] TSIROGIANNIS, E.C., E. DASKALAKIS, M.H. HASSAN, A.M. OMAR and P. BARTOLO P. Ballistic Design and Testing of a Composite Armour Reinforced by CNTs Suitable for Armoured Vehicles. *Defence Technology*, 2023, in press. DOI 10.1016/j.dt.2023.04.013.

[2] LENIHAN, D, W. RONAN, P.E. O'DONOGHUE and S.B. LEEN. A Review of the Integrity of Metallic Vehicle Armour to Projectile Attack. *Proceedings of the Institution of Mechanical Engineers, Part L: Journal of Materials: Design and Applications*, 2019; **233**(1), pp. 73-94. DOI 10.1177/1464420718759704.

[3] PAI, A., M. RODRIGUEZ-MILLAN, M. BEPPU, B. VALVERDE-MARCOS and S. SHENOY. Experimental Techniques for Performance Evaluation of Shielding Materials and Configurations Subjected to Blast and Ballistic Impacts: A State-of-the-Art Review. *Thin-Walled Structures*, 2023, **191**, 111067. DOI 10.1016/j.tws.2023.111067.

[4] PAI, A., C.R. KINI and S. SHENOY. Development of Materials and Structures for Shielding Applications against Blast and Ballistic Impact: A Detailed Review. *Thin-Walled Structures*, 2022, **179**, 109664. DOI 10.1016/j.tws.2022.109664.

[5] ABEBE, S. and T.A. MOHAMMED. Structures under Synergetic Effects of Combined Blast and Impact Loads: A State-of-the-Art Review. *Advances in Civil Engineering*, 2022, **2022**, 6934078. DOI 10.1155/2022/6934078.

[6] PRATOMO, A.N., S.P. SANTOSA, L. GUNAWAN and I.S. PUTRA. Countermeasures Design and Analysis for Occupant Survivability of an Armored Vehicle Subjected to Blast Load. *Journal of Mechanical Science and Technology,* 2020, **34**, pp. 1893-1899. DOI 10.1007/s12206-020-0411-1.

[7] RYBANSKY, M., M. HUBACEK, J. CAPEK, V. KOVARIK and F. DOHNAL. Terrain Passability Mapping in the Czech Republic. *Abstracts of the ICA,* 2023, **6**(215). DOI 10.5194/ica-abs-6-215-2023.

[8] POKONIECZNY, K. and S. BORKOWSKA. Using High Resolution Spatial Data to Develop Military Maps of Passability. In: *Proceedings of the 2019 International Conference on Military Technologies (ICMT)*. Brno, IEEE, 2019. DOI 10.1109/MILTECHS.2019.8870022.

[9] KARTIKEYA, S., PRASAD and N. BHATNAGAR. Finite Element Simulation of Armor Steel used for Blast Protection. *Procedia Structural Integrity*, 2019, **14**, pp. 514-520. DOI 10.1016/j.prostr.2019.05.066.

[10] SŁAWIŃSKI, G., P. MALESA and M. ŚWIERCZEWSKI. Analysis Regarding the Risk of Injuries of Soldiers Inside a Vehicle during Accidents Caused by Improvised Explosive Devices. *Applied Science,* 2019, **9**(19), 4077. DOI 10.3390/app9194077.

[11] GRZEJDA, R., A. PARUS and K. KWIATKOWSKI. Experimental Studies of an Asymmetric Multi-Bolted Connection under Monotonic Loads. *Materials*, 2021, **14**(9), 2353. DOI 10.3390/ma14092353.

[12] *LS-Dyna Manual vol. 1 R.12.0* [online]. [viewed 2023-02-07]. Available from: https://www.dynasupport.com/manuals/ls-dyna-manualsTM 5-855-1 (1986) Fundamentals of protective design for conventional weapons. U.S. Department of the Army, Technical Manual, USA

[13] HILDING, D. Methods for Modelling Air Blast on Structures in LS-Dyna. In: *Nordic LS-DYNA Users' Conference 2016* Gothenburg: DYNAmore Nordic AB, 2016.

[14] SIRIGIRI, V.R.K., V.Y. GUDIGA, U.S. GATTU, G. SUNEESH and K.M. BUDDARAJU. A Review on Johnson Cook Material Model. *Materials Today: Proceedings*, 2022, **62**(6), pp. 3450-3456. DOI 10.1016/j.matpr.2022.04.279.